THE ASTRONOMICAL JOURNAL, 119:953–969, 2000 February

CLOSE APPROACHES OF TRANS-NEPTUNIAN OBJECTS TO PLUTO HAVE LEFT OBSERVABLE SIGNATURES ON THEIR ORBITAL DISTRIBUTION

D. NESVORNÝ AND F. ROIG
Institute of Astronomy and Geophysics, São Paulo University, Av. Miguel Stefano 4200, 04301 São Paulo, Brazil; david@orion.iagusp.usp.br

AND

S. FERRAZ-MELLO
National Observatory, Rio de Janeiro, Brazil
Received 1999 July 21; accepted 1999 November 3

ABSTRACT

It is shown that in addition to four outer planets (Jupiter to Neptune) Pluto should be also taken into account in studies of the orbital dynamics in the trans-Neptunian region. Pluto's effect is particularly large on the orbits in the 2:3 Neptune mean motion resonance. The trajectories found stable over the age of the solar system when only the gravitational effect of four outer planets is considered are often destabilized there in the effect of close Pluto approaches. We estimate that many dynamically primordial bodies moving initially with low to moderate amplitudes in the 2:3 Neptune resonance (semimajor axis 39.45 AU) have been removed from their respective, otherwise stable, locations, when their resonant amplitudes increased in the course of close encounters with Pluto. At large libration amplitude, the orbits became exposed to chaotic changes, and objects were ejected from the 2:3 resonance to Neptune-crossing trajectories. The process of the resonant amplitude excitation was especially efficient for orbits with moderate and large inclinations ($i > 8°$), where more than 50% of the population has been removed in 4×10^9 yr. We estimate that the remaining part of the primordial resonant population at these inclinations should have had its resonant amplitude excited to about 80°. The effect of Pluto on low-inclination orbits is smaller. We have examined the distribution of 33 objects observed on the 2:3 resonant orbits (Plutinos) and found that there could actually exist indications of the above mechanism. The resonant amplitudes of Plutinos are unusually high for $0.15 < e < 0.3$ when compared with randomly generated distribution, and, also, there is only one object (1997 QJ4) on an orbit similar to that of Pluto. In fact, a certain gap may be noticed in the distribution of Plutinos at Pluto's inclination and eccentricity, which, if confirmed by future observations, may be the consequence of Pluto's sweeping effect.
Key words: celestial mechanics, stellar dynamics — Kuiper belt, Oort cloud

1. INTRODUCTION

The existence of a belt of small bodies beyond Neptune has been independently suggested by Edgeworth (1949) and Kuiper (1951)—hereafter we refer to the belt as the Edgeworth-Kuiper belt (EKB). Fernández (1980) proposed that such a belt could be a reservoir of short-period comets whose low inclinations, as was later shown by Duncan, Quinn, & Tremaine (1988), cannot be explained assuming their origin in the isotropic Oort cloud. The first direct observational evidence of the EKB was the discovery of 1992 QB1 by Jewitt & Luu (1993).

The first results on the stability of the trans-Neptunian region were obtained by Levison & Duncan (1993) and Holman & Wisdom (1993) by means of numeric simulations. In later work, Duncan, Levison, & Budd (1995) numerically computed the evolution of four outer planets (Jupiter to Neptune) and 1300 test particles (with initial inclination equal to 1°) over 4×10^9 yr and mapped the stability of orbits in the 32–50 AU semimajor axis interval with the following findings: (1) the stable orbits with perihelion distances q less than 35 AU were found to be associated with the first-order mean motion resonances with Neptune, where the phase-protection mechanism (as in the case of Pluto in the 2:3 resonance; Cohen & Hubbard 1965) and the absence of overlapping inner secular resonances (Morbidelli, Thomas, & Moons 1995) both contribute to orbit preservation; and (2) the unstable orbits with $q > 35$ AU were found to be related to the perihelion and node secular resonances (mainly ν_8, ν_{17}, and ν_{18} located at $40 < a < 42$ AU, according to Knežević et al. 1991).

There are currently registered about 120 EKB objects in the Minor Planet Center catalog.[1] Their orbital distribution is well correlated with the results of Duncan et al. (1995) in the sense that most of them have orbits characterized by long-term stability. Thirty-three of the known EKB objects and Pluto happen to fall in the region of the 2:3 mean motion resonance with Neptune at the semimajor axis $a = 39.45$ AU.

Pluto has a peculiar orbit. It is highly eccentric ($e = 0.25$) with large inclination ($i = 17°$). Its resonant argument $\sigma = 2\lambda_N - 3\lambda + \varpi$, where λ_N is the mean Neptune longitude and λ and ϖ are the mean and perihelion longitudes of Pluto, librates around 180° with $\sim 80°$ amplitude (A_σ) and $\sim$20,000 yr period. In addition to the 2:3 commensurability, Pluto's argument of perihelion (ω) librates about 90° (Williams & Benson 1971). Its amplitude A_ω is approximately 23°, and its period is about 3.8×10^6 yr. The libration of ω is a consequence of Pluto being located in Kozai's secular resonance (Kozai 1962). In addition to the 2:3 and Kozai resonances, there is a commensurability of 1:1 between libration of ω and the circulation of the angle $\Omega - \Omega_N$ (Milani, Nobili, & Carpino 1989), where Ω and Ω_N are the nodal longitudes of Pluto and Neptune, respectively.

[1] At: http://cfa-www.harvard.edu/cfa/ps/lists/TNOs.html.

The long-term stability of Pluto's orbit has been confirmed by Kinoshita & Nakai (1984) and Sussman & Wisdom (1988). It turned out that in spite of the positive maximum Lyapunov exponent ($\sim 10^{-7}$ yr^{-1}) its orbit is stable over the age of the solar system.

The 33 Plutinos sharing the 2:3 resonance with Pluto have eccentricities in the range from 0.08 to 0.35 and inclinations smaller than 20° (only one known resonant object—1996 KY1—has the inclination of about 30°). The orbits of most Plutinos are expected to be stable on long time intervals. The orbital elements of Plutinos are, however, usually not determined with sufficient precision to make the long-term simulations of their orbits meaningful.

Concerning the global stability of the 2:3 Neptune resonance, the works based on averaged circular (Morbidelli et al. 1995) and circular (Malhotra 1996) models indicated that the central resonant space is stable over the age of the solar system, but both were missing an important ingredient—the complete perturbations of outer planets other than Neptune—in order to provide sufficiently reliable stability boundaries. The stability boundaries were as a function of the resonant amplitudes A_σ and A_ω computed for the orbits with Pluto-like inclinations by Levison & Stern (1995). They have found that the orbits starting with $A_\sigma < 50°$ are stable and the orbits with $A_\sigma > 120°$ are unstable over 4×10^9 yr. For intermediate resonant amplitudes A_σ, usually a small amplitude of ω-libration is needed for stabilization of the orbit. The stability of the 2:3 resonance was further investigated by Morbidelli (1997) with the emphasis on a number of escaping objects and their relation to the short-period comets.

We analyze the orbital distribution of Plutinos in § 2 and show that there can actually exist some uncommon features that could have resulted only with difficulty from the secular evolution under the perturbations of four outer planets. Although this observational evidence is based on a small number of known 2:3 resonant objects and their frequently inaccurate orbital elements, we believe that it is worth of examining the possible causes.

Although a number of primordial and collision mechanisms that complicate the matter could had been involved, some of the features of Plutino orbital distribution may be a result of the interaction with Pluto in the past 4×10^9 yr. We conjecture that the small Pluto mass (the total mass of the Pluto-Charon binary is estimated to be $1/1.35 \times 10^8$ of the Sun's mass) can be compensated both by the length of the time interval in question and by the similarity of the orbital parameters of Pluto and Plutinos (§ 3). In order to test this hypothesis we have performed several numeric simulations considering Pluto as the fifth massive body in addition to the four outer planets. The setup and results of our main experiment, in which we place the test particles in the 2:3 and Kozai resonances, are explained in § 3. A simple classification of orbits based on their interaction with Pluto is given in § 4.

We analyze the effect of Pluto on 2:3 resonant orbits and show that it results in an important excitation of the resonant amplitude A_σ. Pluto's effect is especially important on the inclined orbits, and we show that a large number of objects have been removed from the 2:3 resonance in consequence of the excitation of A_σ beyond the stability limits. The surviving part of the 2:3 resonant population should have had the mean A_σ of about 80° (§ 5). The dependence of these results on the eccentricity is studied in § 6.

As this paper was being revised, we learned about the work of Yu & Tremaine (1999). The authors develop a simplified model of Plutino dynamics under the joint effect of Neptune and Pluto. As this work is closely related to the subject of our paper, we will comment on the results of Yu & Tremaine whenever we find it appropriate.

2. PLUTO AND THE ORBITAL DISTRIBUTION OF PLUTINOS

There are Pluto and 33 trans-Neptunian objects (Plutinos) located in the 2:3 mean motion resonance with Neptune that are registered in the Minor Planet Center Catalog at the time of writing of this paper (1999 March). Thirteen (39%) of the Plutinos are objects observed in more than one opposition with the orbital elements determined with good precision. The other 20 Plutinos (61%) are single-opposition objects for which it was assumed in order to allow for the computation of the orbital elements that they were observed at perihelion (i.e., assumed mean anomaly $M = 0$). The mean anomaly computed for the multi-opposition Plutinos is generally nonzero (but usually within $\pm 40°$—with the exception of 1996 RR20, which is far from perihelion with $M = 112\overset{\circ}{.}3$). This means, as the distribution of Plutinos in the mean anomaly should be the same for single- and multiopposition objects, that the orbital elements of single-opposition Plutinos are generally imprecise, and for some of them the determination of the orbital elements may be wrong as the assumption on their present M can turn out to be invalid. The sizes of known Plutinos range between 50 and 300 km in diameter and are fairly uncertain owing to unknown albedos.

Jewitt, Luu, & Trujillo (1998) estimate on the basis of the current discovery rate that there are between 7000 and 14,000 objects larger than 100 km in diameter in the 2:3 Neptune mean motion resonance. The observations are providing new EKB objects with an increasing discovery rate, and it is clear that there will be soon available an extensive database of Plutinos' orbital and physical characteristics. The question is, however, whether there is something that can be inferred on the orbital distribution of Plutinos at present, from the orbital properties of the 33 observed bodies. We will show in the following that the population of 2:3 resonant objects really differs in several aspects from what would be expected to be an initially random distribution shaped by the long-term gravitation effect of four outer planets.

We have started our analysis by advancing Pluto and 33 Plutinos to the same date: 1999 January 22 (MJD 2,451,200.5). First, the four outer planets (Jupiter to Neptune) were propagated to the catalog date of each object, and then, each object was individually integrated as a massless particle with four outer planets up to the destination time. Even if the integration time was at most only 1960 days, this procedure cannot be substituted by a shift of M according to the mean motion because the short periodic perturbations of Jupiter cause variations of semimajor axis of some Plutinos as large as 0.08 AU with a periodicity of 11.8 yr.

In order to suppress the short periodic variations of Plutino trajectories and retain the resonant and secular variations, we have applied the digital filter of Quinn, Tremaine, & Duncan (1991) in the following experiment. In this experiment, Pluto and Plutinos were integrated with four outer planets for 10^7 yr using the symmetric multistep integrator of Quinlan & Tremaine (1990). The time step for the integration was less than 0.1% of the orbital period so that no spurious instabilities should have been created by low-order resonances between the time step and the dynamical frequencies. Tests have also been done changing the time step. The filtering procedure was sequentially applied 3 times on the integration output increasing the sampling interval at each step from the initial 2 to the final 200 yr. All periods shorter than 1200 yr were suppressed by a factor of 10^5 in amplitude, and the periods larger than 2000 yr were retained in the filtered signal. The filtered elements were $a \exp \imath\sigma$, $e \exp \imath\varpi$, and $i \exp \imath\Omega$ (i is the orbital inclination and $\imath = \sqrt{-1}$).

The purpose of this integration was in numeric determination of the orbital elements that would characterize the properties of the resonant and secular motions of Plutinos. The instantaneous (osculating) orbital elements a, e, and i on 1999 January 22 were not suitable for this purpose because of the following reason. Assume a Plutino to have the same amplitudes A_σ, A_ω and the same "mean" inclination as Pluto, but a phase difference in σ and ω from Pluto's resonant angle and perihelion argument on 1999 January 22. Plutino's instantaneous orbital elements a, e, and i on 1999 January 22 were then considerably different from the orbital elements of Pluto on this date, in spite of both orbits having the same resonant and secular evolutions.

There are a number of different approaches to this problem. In the case of a motion in the mean motion resonance, the *proper* orbital elements can be defined as the values of instantaneous a, e, and i at intersections of a trajectory with some phase space manifold (Nesvorný & Ferraz-Mello 1997), as the maximum or minimum values of instantaneous a, e, and i over a long time interval (Morbidelli 1997) or as amplitudes of resonant angles computed as the maximum excursion of the resonant angles from the libration centers (Levison & Stern 1995).

Following the approach of Nesvorný & Ferraz-Mello (1997) the natural choice of the manifold is $\sigma = 180°$ and $\omega = 90°$ as these values correspond to the libration centers of the 2:3 and Kozai resonances. The behavior of trajectories in the 2:3 and Kozai resonances (Morbidelli et al. 1995) is such that the instantaneous orbital elements a and e oscillate with σ while the e and i change is correlated with ω. When $\sigma = 180°$ both a and e are at the extrema of their resonant oscillations, a having the value corresponding to the maximum excursion from the center of the 2:3 resonance. When $\omega = 90°$, i is also at the maximum excursion from the center of the Kozai resonance.

In Figure 1 we show the semimajor axis, eccentricity, and inclination of Pluto and Plutinos at the first intersection of their trajectories with $\sigma = 180°$ and $\omega = 90°$ (or $\omega = 270°$—the value corresponding to the second libration center of the Kozai resonance; see Morbidelli et al. 1995—if there is no intersection with $\omega = 90°$ within 10^7 yr). The open circles in Figure 1 are the multiopposition Plutinos, the dots are the single-opposition objects, and the circled plus sign marks the position of Pluto. As we consider the first intersection, there is one symbol per object in Figure 1. Owing to the symmetry of the 2:3 resonance with respect to the libration centers, the next intersection of an orbit with $\sigma = 180°$ would be symmetrically placed in the opposite half-plane of the 2:3 resonance in Figure 1*a*. A similar symmetry holds for the orbits with the libration of ω for which the next intersection of $\omega = 90°$ would occur in the opposite half-plane of the Kozai resonance in Figure 1*b*.

The bold lines in Figure 1*a* are the separatrices and libration centers of the 2:3 resonance. Other lines in the figure show the positions of the secular resonances (ν_8, ν_{18}, and Kozai resonance denoted by ω) and the secondary resonance 5:1, where the resonant frequency is a factor of 5 larger than the frequency of the perihelion longitude. Other secondary resonances, where the integer ratios of the resonant and perihelion frequencies are smaller, are located at lower eccentricities under the dotted line of the 5:1 secondary resonance. The bold lines in Figure 1*b* are separatrices of the Kozai resonance, and the dotted line shows the libration centers of ω. Locations of the resonances and their separatrices have been computed by Thomas (1998) following the seminumeric method of Henrard (1990).

Most of the Plutinos are located at $39.25 < a < 39.7$ AU and $0.08 < e < 0.35$ in Figure 1*a*. In this central area of the 2:3 resonance, the orbits are stable over the age of the solar system (Morbidelli 1997). This is in agreement with the presumption that the observed Plutinos are long-lived 2:3

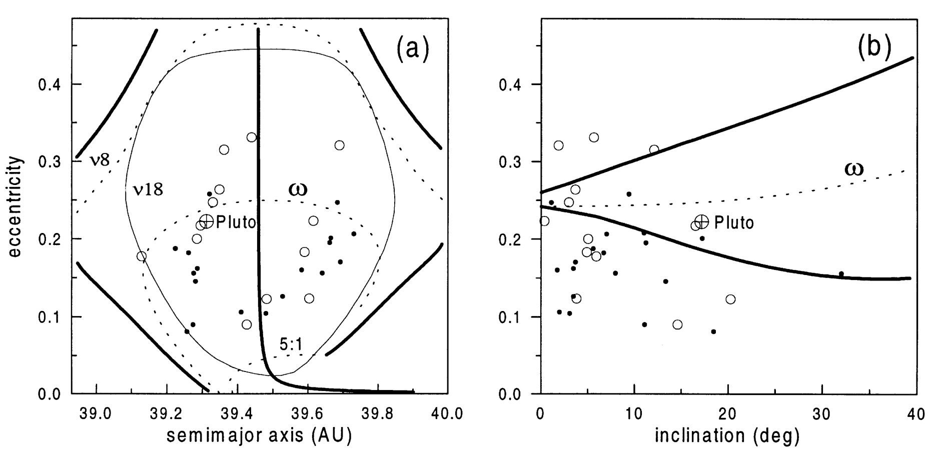

FIG. 1.—Orbital elements of Pluto (*circled plus sign*), multiopposition (*open circles*) and single-opposition Plutinos (*dots*) at the time when their $\sigma = 180°$ and $\omega = 90°$. The separatrices and libration centers of the 2:3 Neptune resonance are shown by bold lines in (*a*). The other lines denote the locations of the secular (ω-libration in Kozai resonance, ν_8 and ν_{18}) and secondary resonances (5:1). The bold lines in (*b*) show the location of the separatrices of the Kozai resonance; the dashed line denoted by ω is its libration center. In (*a*), note the lack of objects near the libration centers of the 2:3 resonance ($a = 39.45$ AU) for $0.15 < e < 0.3$. In (*b*), there are few objects with orbital characteristics similar to Pluto's orbit, and among them only 1997 QJ4 has a well-determined and stable orbit.

resonant objects. The resonant orbits are unstable outside the above semimajor axis limits owing to the simultaneous presence of the ν_{18}, ν_8, and Kozai secular resonances at large libration amplitudes $A_\sigma > 130°$. According to Nesvorný & Roig (2000) there exists another instability under the line of the 5:1 secondary resonance owing to the overlap of the 2:1, 3:1, and 4:1 secondary resonances. No resonant objects are known with $e < 0.08$ (Fig. 1*a*). The orbits with eccentricities larger than 0.35 are also unstable. There are the overlapping ν_8 and ν_{18} secular resonances that destabilize motion there, and moreover, the orbital perihelion is already close to the orbit of Uranus ($a_U = 19.22$ AU) for these eccentricities. No resonant objects with $e > 0.35$ have been discovered until now.

What is surprising concerning the Plutino distribution in Figure 1*a* is that in the interval $0.15 < e < 0.3$ there are no objects close to the libration centers (bold vertical line at $a = 39.5$ AU). The orbits of such objects would be characterized by small resonant amplitudes $A_\sigma < 50°$ and the stability over the age of the solar system according to the results of Morbidelli (1997).

The inclinations of most Plutinos are lower than 10°, and there is only one object, 1996 RR20 (observed in one opposition), with an inclination larger than 20° (Fig. 1*b*). According to Nesvorný & Roig (2000) the resonant orbits with large inclinations $20° < i < 30°$ are stable over the age of the solar system. There is, however, a large observational incompleteness at these inclinations, which means that how fast the real density of Plutinos decreases with inclination can only be shown by future observational searches specifically directed to this subject.

The resonant object, the symbol for which overlaps the symbol of Pluto in both panels of Figure 1, is the multi-opposition Plutino 1997 QJ4. Its orbital evolution is apparently very similar to that of Pluto. The absolute magnitude of this body is 7.5, which means a diameter between 85 km (for 0.25 albedo) and 200 km (for 0.05 albedo). The other object that appears close to Pluto's position in Figure 1*b* is 1998 WW24 (the point at $e = 0.2$ and $i = 17°$). This is a single-opposition object with large resonant amplitude $A_\sigma = 115°$ and is actually not in the Kozai resonance (the separatrices of the Kozai resonance in Fig. 1*b* were computed for $A_\sigma = 0$). Another object, the single-opposition 1997 TX8 with $i \sim 10°$ close to the libration center of the Kozai resonance (dotted line in Fig. 1*b*), was found unstable in our integration owing to its initially large A_σ. The fact that this objects escapes from the 2:3 resonance in less than 10^7 yr suggests that the orbital elements of this body were not correctly determined from the observation (otherwise the flux of escaping bodies from the 2:3 resonance would be unacceptably large).

Consequently, among 33 known Plutinos, only 1997 QJ4 has an orbit with characteristics similar to Pluto's orbit. In fact, a gap may be noted around Pluto in the distribution of Plutinos in Figure 1*b*. This gap roughly coincides with the area of Kozai resonance for $i > 5°$ and is probably somewhat larger for the inclinations comparable with Pluto's inclination ($i = 17°$). Levison & Stern (1995) computed that with four outer planets, the orbits at low resonant amplitudes A_σ and A_ω are stable, so that, if real, this gap could be attributed to Pluto's own gravitational effect rather than to the effect of four outer planets.

We show in Table 1 the amplitudes A_σ and A_ω of four Plutinos (and Pluto) found with stable ω-libration in 10^7 yr.

TABLE 1

PLUTO AND FOUR PLUTINOS WITH STABLE LIBRATIONS OF THE ARGUMENT OF PERIHELION IN 10^7 YR

Object (1)	$\langle i \rangle$ (deg) (2)	A_σ (deg) (3)	A_ω (deg) (4)
Pluto	15.9	84.9	22.9
1997 QJ4	15.8	98.5	27.6
1998 UU43	11.6	80.6	47.9
1994 TB	16.7	55.2	73.1
1996 SZ4	6.4	90.6	79.2

NOTE.—Col. (2): Mean inclination. Col. (3): Amplitude of σ (A_σ). Col. (4): Amplitude of ω.

All but 1998 UU43 have the center of ω-libration at 90°. 1998 UU43 oscillates about 270°.

The perihelion argument of Pluto and 1997 QJ4 oscillates around 90° with low amplitude, while ω of 1998 UU43 oscillates about 270°. 1994 TB and 1996 SZ4 are very close to separatrices (their ω starts to alternate between libration and circulation soon after 10^7 yr). All these Plutinos were observed in more than one opposition.

The maximum eccentricity versus A_σ, the latter being computed as the maximum excursion of σ from 180° on a 10^7 yr interval, is shown in Figure 2*a*. Triangles are the Plutinos with inclination smaller than 10°, and plus signs are the Plutinos with $i > 10°$. Two single-opposition objects (1996 KY1 and 1997 TX8) escaped from the 2:3 resonance on this interval, probably owing to the imprecise determination of their initial orbital elements from few observations. Two multiopposition objects (1993 RO and 1996 RR20) have A_σ larger than 120° (128° and 124°, respectively) and are probably unstable in the long run.

For $0.15 < e < 0.3$ in Figure 2*a* there is only one Plutino with $A_\sigma < 70°$ (no such object for $0.2 < e < 0.3$), which is, as already noted in Figure 1*a*, a rather surprising underpopulation of stable low-A_σ orbits. To assure that the lack of resonant objects at low A_σ is significant, we have performed the following test.

The initial orbital elements of 150 test particles have been randomly chosen with $39 < a < 39.8$ AU, $0.1 < e < 0.35$, and $i < 20°$, and A_σ was determined for them by the same procedure as for the real resonant objects (i.e., as the maximum excursion from 180° in 10^7 yr). In Figure 2*b*, we compare the cumulative number of real ($0.15 < e < 0.3$) and randomly generated bodies versus A_σ. The number of test particles was rescaled to 20 objects with $A_\sigma < 130°$, which is the cumulative number of real Plutinos at this limit.

The cumulative number of test particles linearly increases with the libration amplitude with a characteristic slope. We have verified that this slope is a robust feature of random distributions of orbits in the 2:3 resonance. The real distribution considerably differs from the random one. While for $A_\sigma < 70°$ the cumulative number of real Plutinos increases less steeply with increasing A_σ, for $A_\sigma > 70°$, the slope is steeper than the random one owing e to a relative surplus of real Plutinos with these libration amplitudes. In contrast to the distribution of real Plutinos, the random distribution indicates that about 25% of objects (five of 20 objects) with $A_\sigma < 130°$ should have $A_\sigma < 70°$.

Even if the final conclusion is due to a fairly uncertain small sample of known resonant objects, we believe that there actually exist indications in the observed orbital

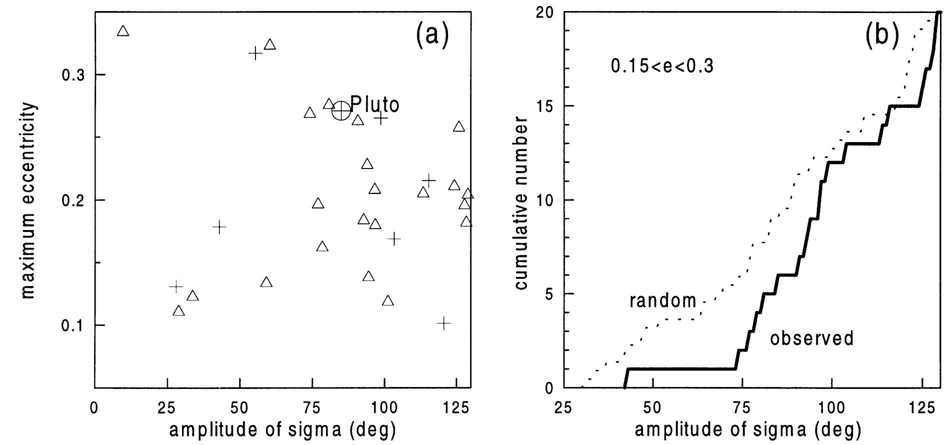

FIG. 2.—(*a*) Maximum eccentricity vs. the amplitude of the resonant angle A_σ, both being computed on 10^7 yr interval. Plutinos with $i < 10°$ are denoted by triangles and those with $i > 10°$ by plus signs. Pluto's orbit is marked by a circled plus sign. There is an apparent lack of objects with $A_\sigma < 70°$ for $0.15 < e < 0.3$. In (*b*) we compare the cumulative number of known Plutionos having the resonant amplitude smaller than A_σ (*solid line*) with a randomly generated distribution (*dotted line*). For $A_\sigma < 70°$ there are 5 times fewer Plutinos than the randomly generated bodies. This difference is interesting as it cannot be explained by the dynamical clearing of low-A_σ region under the effect of four outer planets.

distribution of Plutinos that suggest that their resonant amplitudes were excited to values larger than 70° in the past. This fact, together with the lack of the 2:3 resonant objects with orbits similar to Pluto in the Kozai resonance, are the two observational results we would like to address in the following.

3. PLUTO'S INTERACTION WITH THE 2:3 RESONANT OBJECTS

We assume that Pluto's orbit is ancient. Although how its elongated and inclined orbit were formed is a debatable question (Malhotra 1993; Levison, Stern, & Duncan 1999; Petit, Morbidelli, & Valsecchi 1999), it is agreed that this happened at least some 4×10^9 yr ago. We also assume that the gravitational pull of this planet was in the past 4×10^9 yr proportional to the mass of $1/1.35 \times 10^8$ fraction of the Sun's mass, which is about the best estimate of the total mass of Pluto-Charon binary based on *Hubble Space Telescope* (*HST*) observations (see Stern & Yelle 1999). The question is then what are the possible consequences of Pluto's sweeping through the 2:3 resonant region.

A question related to this subject was addressed by Levison & Stern (1995). They studied the early dynamical evolution of the Pluto-Charon binary under the effect of other 2:3 resonant bodies and suggested the possible origin of Pluto's uncommon heliocentric orbit. Here, however, we are more interested in the opposite case of Pluto's interaction with the resonant objects as a possible effect of Pluto's gravitational scattering on the 2:3 resonant population.

According to Morbidelli (1997), the low-amplitude 2:3 resonant orbits are stable for $0.1 < e < 0.3$ in the model with four outer planets (Jupiter to Neptune) in the sense that they do not leave the resonance in 4×10^9 yr. Even if the range of stable resonant orbits spans a slightly larger interval in eccentricities, for $0.1 < e < 0.3$ and $A_\sigma < 50$, the orbits are not only stable against ejection by four outer planets, but moreover, as their proper elements are almost constant on 4×10^9 yr (Morbidelli 1997), the orbits do not chaotically evolve with time. This moderate eccentricity and low-A_σ resonant region is an ideal testing place for Pluto's hypothetical effect. The secular changes of proper orbital elements in the model with the gravitational perturbations of four outer planets and Pluto must be attributed to Pluto's own effect there.

Moreover, according to the previous section there exists a strong motivation for a study of Pluto's effect on the resonant low-A_σ orbits, which is the lack of objects observed on such orbits. There should exist a mechanism other than the gravitational effect of the outer planets that removed the resonant objects from there, presumably by an excitation of their resonant amplitudes. Assuming that the lack of low-A_σ Plutinos is not dynamically primordial, we suspect two possible mechanisms of long-term excitation of A_σ: either the excitation in mutual encounters and collisions between the 2:3 resonant objects or the effect of close encounters between the resonant objects and Pluto. As the excitation happens mainly in $0.15 < e < 0.3$, we rather think the second mechanism to be at work. Indeed, Pluto has a mean eccentricity of 0.253, which places it close to the center of the above interval.

In order to estimate the possible long-term effect of Pluto on other 2:3 resonant objects, we have performed several simulations of different sets of initial conditions for time intervals ranging from 10^9 to 4×10^9 yr. Pluto has been included in these simulations as the fifth perturber (in addition to four outer planets) with a mass of $\mu = 1/1.35 \times 10^8$ solar masses. This mass is so low that the only expected effect on other resonant bodies presumably happens only when an object approaches Pluto at a small distance. The important quantity is then the radius of the Hill sphere of Pluto, which is given by

$$R_{\rm H} = a_{\rm P}\left(\frac{\mu}{3}\right)^{1/3} = 0.054 \text{ AU} , \quad (1)$$

where $a_{\rm P}$ is the semimajor axis of Pluto. This radius is equal to the distance from Pluto to the collinear stationary point in the circular model of the Sun–Pluto–test particle system. The sphere with Hill radius roughly delimits the space where Pluto's effect on the third body is important. In our case, the corresponding diameter of the zone of Pluto's influence is roughly the size of the central 2:3 resonant region, where $A_\sigma < 50°$.

The result of an encounter with Pluto depends on the mutual velocity V between the object and Pluto. According to Öpik (1976), a trajectory passing close to Pluto bends with an angle γ (deflection angle) between the asymptotes of the incoming and outgoing trajectories given by

$$\tan \frac{\gamma}{2} = (2\pi)^2 \frac{\mu}{bV^2} , \quad (2)$$

where $\mu = 1/1.35 \times 10^8$ and b is the minimum distance between the *unperturbed* path of the particle and Pluto, i.e., the path that would be followed if the planet had no mass (V is given in AU yr^{-1} and b in AU). The deflection angle scales as $1/V^2$. If V is small, then the deflection angle is large, and so is the expected change of the orbital elements. Owing to the large inclination of Pluto (17°), there exists a relatively large lower threshold of the mutual encounter velocity with the *low*-inclination orbits dictated by the mutual inclination of the intersecting trajectories. The changes of orbital elements and in particular of A_σ are expected to be small in this case. Indeed, our preliminary numerical simulation[2] of Pluto's effect on the low-inclination resonant orbits showed that the excitation of A_σ for the initially low-A_σ orbits is relatively small and accounts for at most 20° change of A_σ of individual test particles on 5×10^8 yr.

We have also noticed a weak dependence of $A_\sigma(t = 10^9$ yr) on the initial eccentricity in this experiment. The resonant amplitude excitation for the orbits initially with $e < 0.15$ was a factor 1.5 larger than the change of A_σ for $e > 0.2$. Yu & Tremaine (1999) suggested that Pluto's effect should be small for low-eccentricity orbits owing to larger mutual velocity between the test particles and Pluto. Indeed, the mutual velocity of two bodies at the encounter can be inferred from simple geometric considerations. Suppose Pluto's orbit is fixed with $a_P = 39.45$ AU, $e_P = 0.25$, $i_P = 17°$, and $\omega_P = 90°$. An object on a planar orbit of the same semimajor axis encounters Pluto at either the descending or ascending node of Pluto's orbit. Choosing the line between the Sun and Pluto's ascending node to be the reference axis, we have as a necessary condition for the intersection of both trajectories that object's perihelion longitude ϖ is

$$\varpi = \pm \frac{1}{e} \frac{e^2 - e_P^2}{1 - e_P^2} , \quad (3)$$

with the sign plus for the intersection in Pluto's ascending node and the sign minus for the intersection in Pluto's descending node. No intersection exist when $e < e_P^2 = 0.0625$ because in this case the perihelion distance of the object is larger than the heliocentric distances of Pluto's nodes. The mutual encounter velocity V is a function of the eccentricity e. For $e = 0.1$ the velocity is $V = 0.35$ AU yr^{-1}, and for $e = 0.25$ it is $V = 0.3$ AU yr^{-1}. The minimum encounter velocity of 0.3 AU yr^{-1} when both orbits have the same eccentricity is due to their mutual inclination.

Apart from the velocity the other important factor is the frequency of mutual encounters between test particles and Pluto. We have registered 5900 encounters within R_H to Pluto in 10^9 yr in our experiment. The number of encounters per particle varies with eccentricity. While at $e = 0.1$ it is about 40, at $e = 0.25$ it is only 20. This is probably the reason that the excitation of the libration amplitude is moderately larger at $e = 0.1$ than at $e = 0.25$ in our experiment, contrary to what would be expected from the encounter velocities. The cumulative deflection angle expected at $e = 0.1$ should be, according to the above results, a factor $40 \times 0.3^2/20 \times 0.35^2 = 1.5$ larger than the cumulative deflection angle at $e = 0.25$. The larger cumulative deflection angle translates to a larger excitation of A_σ at $e = 0.1$ observed in our experiment.

It may be inferred from the above considerations that the orbits with nonzero inclinations should suffer larger changes at encounters with Pluto's than the orbits with zero inclination. On the other hand, however, even an orbit with $i = i_P$ can have a large encounter velocity at the intersection if the nodes of both orbits are not aligned. There is an additional factor to be noted at this point.

Assuming the orbit of the Plutino with $a = 39.45$ AU and $e \sim e_P$, then this orbit is resonant both in the 2:3 mean motion resonance with Neptune and in the Kozai secular resonance. Assuming additionally that both libration amplitudes A_σ and A_ω of the Plutino orbit are zero and in an idealized case in which Pluto's orbit also has $A_\sigma^P = A_\omega^P = 0$, then $\sigma = \sigma_P = 180°$ and $\omega = \omega_P = 90°$, where the index P denotes the quantities of Pluto. These conditions result in the following relation between the mean longitudes and nodes:

$$\lambda - \lambda_P = \tfrac{1}{3}(\Omega - \Omega_P) . \quad (4)$$

This means, as the arguments of perihelion are fixed at 90°, that the orbits intersect each other only if $\Omega = \Omega_P$. At such an instant, the close encounters become possible also as $\lambda = \lambda_P$. We therefore conclude that the only necessary (and sufficient) condition to be satisfied in order to have close and low-velocity encounters between Pluto and the resonant objects in the Kozai resonance is the alignment of nodes. The encounters at nodes are characterized by a velocity V proportional to $|\Delta i| = |i - i_P|$. Equation (4) will hold true on average even if the libration amplitudes are nonzero.

The motion of the nodal line of Pluto's orbit is retrograde and has a period of 3.8×10^6 yr. A Plutino on an orbit similar to that of Pluto naturally has a similar nodal period. Consequently, the differential rotation of nodes between Pluto and Plutino orbits will be very slow. The numeric integration shows that if there is no interaction between Pluto and Plutino, then $\Omega - \Omega_P$ has a period larger than 10^8 yr if $|\Delta i|$ is of order of a few degrees. The rotation of $\Omega - \Omega_P$ is prograde when $\Delta i > 0$ and retrograde when $\Delta i < 0$. Consequently, the period of many close encounters between Pluto and Plutino when $\Omega - \Omega_P = 0$ will be followed by a long period of time in which the Plutino orbit is protected from close encounters as $\lambda - \lambda_P \neq 0$.

4. ESCAPES FROM INITIALLY LOW-A_σ AND LOW-A_ω ORBITS

We have simulated the evolution of 101 test particles that were initially placed on the ω-librating orbits in the 2:3 mean motion resonance with Neptune. The initial elements were chosen so that both the libration amplitudes of ω and of σ of the particles were initially close to zero. The semi-

[2] The setup of this preliminary simulation was the same as for the experiment described in detail in the next section. Initially, $i = 2°$ for all test particles.

major axis and eccentricity were set to 39.2 AU and 0.25, and inclination was varied between 5° and 25° with a 0°.2 step. The initial angles were chosen so that $\sigma = 180°$, $\omega = 90°$, and $\Omega - \Omega_N = 0$, where Ω_N is the node longitude of Neptune.

As determined prior to the simulation, the initial osculating semimajor axis of 39.2 AU corresponds to the initial mean semimajor axis of 39.45 AU (the value of the 2:3 libration centers—Fig. 1*a*) for the configuration of planets on 1998 January 1 (MJD 2,450,814.5). The difference between the initial orbital and mean values of semimajor axes is a consequence of the short period variations of test particles orbits. Hence, the test particles were chosen within a small interval around the stable libration center of the 2:3 Neptune resonance with a corresponding libration amplitude of the resonant angle $\sigma = 2\lambda_N - 3\lambda + \varpi$ smaller than 20°.

The initial conditions of four major planets and Pluto were taken on 1998 January 1 (MJD 2,450,814.5) with respect to the invariant plane and equinox at epoch JD 2000. The orbits of five planets (massive bodies) and test particles (massless bodies) were followed forward in time using the swift_rmvs3 integrator of Levison & Duncan (1994) and a 1 yr time step. The total integration time span was 4×10^9 yr. The orbital elements were computed each 10^5 yr. For each test particle in the run we calculated the resonant amplitude A_σ at time t as the maximum excursion of σ from 180° in the interval $(t, t + 10^7)$ yr and the amplitude A_ω as the maximum excursion of ω from 90° on the same interval. We also calculated the proper eccentricities and inclinations at time t as the averages of orbital elements in the interval $(t, t + 10^7)$ yr (Morbidelli & Nesvorný 1999, their eq. [1]).

During the simulation we have monitored A_σ, and if this happened to exceed 175°, we classified the corresponding case as the escape from the 2:3 resonance. The test particle may then, however, survive a relatively long interval ($< 10^8$ yr) chaotically diffusing on the resonant border before the first important encounter with Neptune. The subsequent evolution under the effect of close encounters with giant planets was faster, and in an interval typically of order of 10^7 yr, the test particle was deactivated from the run. The test particle was deactivated when its orbit satisfied one of our stopping criteria: either too close an encounter to some giant planet or to the Sun, or ejection to a heliocentric distance larger than 100 AU. The behavior of bodies escaping from EKB and becoming giant-planet crossers was studied in detail by Levison & Duncan (1997).

Many test particles had escaped from the 2:3 Neptune resonance in the run (Fig. 3). The cumulative number of escapes is roughly a linear function of time with about 13 escapes per 10^9 yr. This resulted in total of 51 escaping particles in 4×10^9 yr.

While both the proper eccentricity and the proper inclination remained basically the same in the initial stages of evolution, the resonant amplitude A_σ of test particles increased. The final resonant amplitude $A_\sigma(4 \times 10^9$ yr) is shown in Figure 4*a* (*shadow bars*) versus the initial proper inclination (both computed on 10^7 yr interval). For the test particles escaping from the resonance before 4×10^9 yr, the quantity shown is 180°. The solid line denotes the initial resonant amplitude $A_\sigma(0)$. The horizontal line at $A_\sigma = 130°$ is given for reference, since for $A_\sigma > 130°$, the orbits are chaotic and diffuse quickly toward the borders of the 2:3

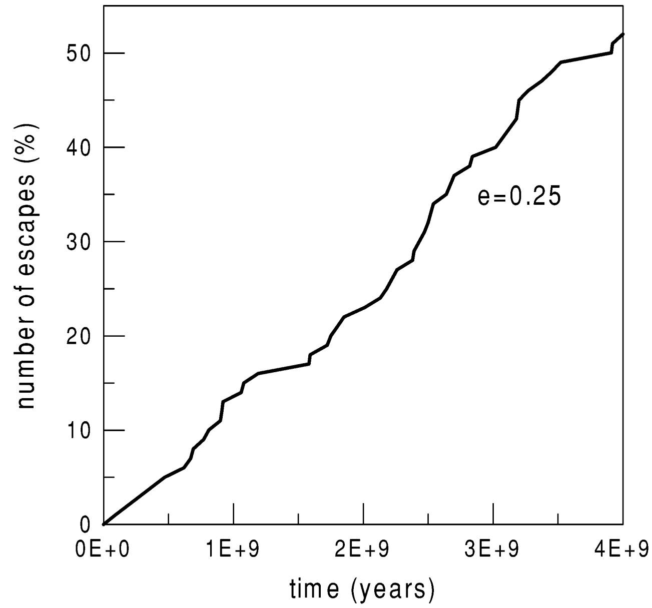

FIG. 3.—Cumulative number of escaping test particles from the 2:3 resonance. More than 50% of initially low-A_σ and low-A_ω ($e = 0.25$) test particles left the resonance before $t = 4 \times 10^9$ yr when their resonant amplitude increased beyond the instability limit.

resonance under the effect of four outer planets (Morbidelli 1997).

There is no strong dependence of $A_\sigma(4 \times 10^9$ yr) on the initial proper inclination observed in Figure 4*a*. Note, however, that the excitation of A_σ was moderately smaller

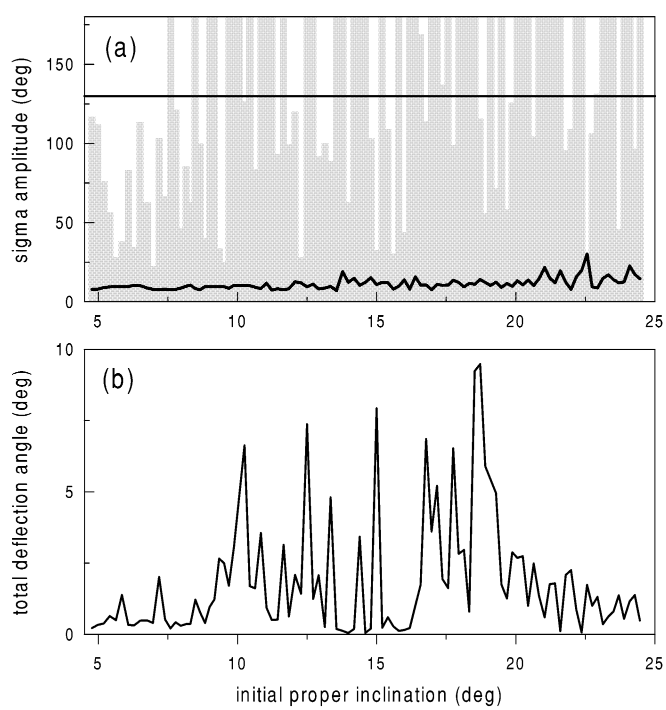

FIG. 4.—(*a*) Initial (*solid line*) and final (*shadow bars*) resonant amplitude A_σ observed in the simulation of test particles placed in the Kozai resonance with $e = 0.25$. The horizontal line at $A_\sigma = 130°$ shows an approximate limit where orbits are unstable owing to the effect of four outer planets. (*b*) Total deflection angle resulting from the encounters of test particles with Pluto in 4×10^9 yr. Öpik two-body approximation of encounters was used for its computation. See text for discussion.

at low inclinations. There were no escapes for $i < 7\rlap{.}^{\circ}5$, presumably because the mutual velocities of Pluto–test particle encounters were enhanced there by larger mutual inclination of their respective orbits, which rendered the encounters ineffective. Note on the other hand that only 12 (25%) of the test particles survived with $A_{\sigma} < 130^{\circ}$ for $16^{\circ} < i < 25^{\circ}$.

The excitation of A_{σ} observed in our simulation should be attributed to the gravitational effect of Pluto at close encounters. We have at least three reasons to believe this:

1. We have checked by a 10^9 yr integration that no excitation happened when only four outer planets (without Pluto) are considered in the integration. Initial and final A_{σ} were practically the same in this experiment for all test particles. Consequently, there is no A_{σ} enlargement without Pluto.

2. The swift_rmvs3 integrator was simulating the effect of the Pluto encounters correctly since the 5×10^8 yr integration with the Bulirsh-Stoer integrator gave roughly the same result. We have simulated the orbital evolution of 11 test particles at $9^{\circ} < i < 11^{\circ}$ and of 11 particles at $16^{\circ} < i < 18^{\circ}$. The mean excitation of A_{σ} on this time interval computed by Bulirsh-Stoer was 20% smaller than the one computed by Swift for $9^{\circ} < i < 11^{\circ}$ and was equal to the one computed by Swift for $16^{\circ} < i < 18^{\circ}$. The particle starting at $i = 9\rlap{.}^{\circ}2$ that escaped from the 2:3 resonance at $t = 3.5 \times 10^8$ yr in the simulation with swift_rmvs3, escaped also in the integration with Bulirsh-Stoer at $t = 3.2 \times 10^8$ yr. Considering the irreproducibility of a chaotic trajectory, such a coincidence is even surprising. The Bulirsh-Stoer routine treated close encounters with excellent precision, and we believe that the excitation of A_{σ} was correctly evaluated by this integration method. Consequently, the result of Swift was exact for $16^{\circ} < i < 18^{\circ}$ and the precision of this integration routine slightly degraded (within acceptable limits) for inclinations $\sim 10^{\circ}$. We have further checked that the precision of Swift worsened for initially zero inclinations. While the Bulirsh-Stoer integrator indicated a small ($\sim 10^{\circ}$) excitation of mean A_{σ} in 10^9 yr, the swift_rmvs3 method computed about double of this value. This presumably happened because of an inappropriate step size management of swift_rmvs3 at encounters and the consequent failure in energy conservation. Our tentative explanation of why Swift commits such a large error for low inclinations while being precise for the inclinations comparable to Pluto's is as follows. The physical effect of Pluto is, according to equation (2), proportional to $1/V^2$ and is large for large inclinations (low Pluto-particle mutual inclination). For low inclinations (large Pluto-particle mutual inclination), in a high-velocity regime of encounters, the physical effect of Pluto steeply decreases. From the above experience, we have reason to believe that swift_rmvs3 numerical errors at close encounters have different, less steep dependence on the mutual velocity than $1/V^2$ and are important only for high-velocity encounters.

3. For each encounter of a test particle with Pluto registered by the integrator, we compute the deflection angle and the change of orbital elements following equation (2) and a simple procedure described below, and these estimates are in qualitative agreement with the real simulation (we give an example of that later in Figs. 7 and 9 for the trajectory starting with $i = 11\rlap{.}^{\circ}8$).

The change of orbital elements due to the encounter may by computed in a two-body Öpik approximation. When a test particle is about the distance $R_{\rm H}$ from Pluto, we evaluate from the mutual velocity and position of the test particle and Pluto the energy and angular momentum of the Plutocentric particle's orbit, neglecting the effect all other massive bodies. The particle's hyperbolic orbit is then uniquely defined as is the velocity of the outgoing trajectory at the intersection with the Hill sphere. The difference in heliocentric orbital elements computed at the points at which the incoming and outgoing trajectories intersect the Hill sphere is a measure of the orbital change at the close encounter. It is well known that the result of this computation strongly depends on the size of the sphere around a planet chosen for the computation, and as $R_{\rm H}$ is not the only choice, the real orbital change cannot be precisely computed. We use the two-body approximation for the interpretation of the results obtained by exact numeric simulations.

Figure 4*b* shows the cumulative deflection angle of the test particles that has been obtained by summing the deflection angles computed in the two-body approximations (eq. [2]) of all encounters of a test particle to Pluto during its lifetime (equal to 4×10^9 yr or the time when being deactivated). There is a rough correspondence between Figures 4*a* and 4*b*. First of all, the test particles starting at low inclinations have a small cumulative deflection of order of 1°. The effect of close encounters was apparently not sufficient for large excitation of their A_{σ}. Then there is the interval $9^{\circ} < i < 13^{\circ}$, where the cumulative deflection angle is as large as few degrees. The excitation of the resonant amplitude is larger for these inclinations, and many test particles initially falling into this interval of inclination escaped.

For the initial inclinations of about 15°, the situation is unclear as the cumulative deflection was less than 1° (with two exceptions). There were, however, several escapes at this interval in the exact simulation. The four surviving test particles in the range $13\rlap{.}^{\circ}5 < i < 16\rlap{.}^{\circ}5$ had been protected from close encounters with Pluto for most of the time of simulation. Their orbital dynamics resembled the motion near the leading and trailing Lagrangian points of the Sun–Pluto–test particle system (tadpole orbits—see Brown & Shook 1966). The test particles starting at larger inclination were with few exceptions ejected from the resonance. Their small relative orbital inclination with respect to the orbit of Pluto apparently enhanced the impact of close encounters.

5. TYPES OF ORBITAL BEHAVIOR

The graph of the cumulative deflection angle (Fig. 4*b*) may be interpreted in terms of the frequency and mutual velocity of encounters. In Figure 5*a* we show the number of encounters of test particles within $R_{\rm H}$ to Pluto in the first 3×10^8 yr of our simulation. Figure 5*b* shows the mean mutual velocity between the test particles and Pluto computed over the same time interval. There are on average 10 encounters within one Hill radius to Pluto in 3×10^8 yr.

Without much stress on precision we divide the integrated range of inclination into five intervals (Fig. 5), each of them being characterized by different dynamics and the interaction with Pluto.

5.1. $5^{\circ} < i < 9^{\circ}$

For $5^{\circ} < i < 9^{\circ}$, there were typically only five encounters per particle within one Hill radius to Pluto in 3×10^8 yr,

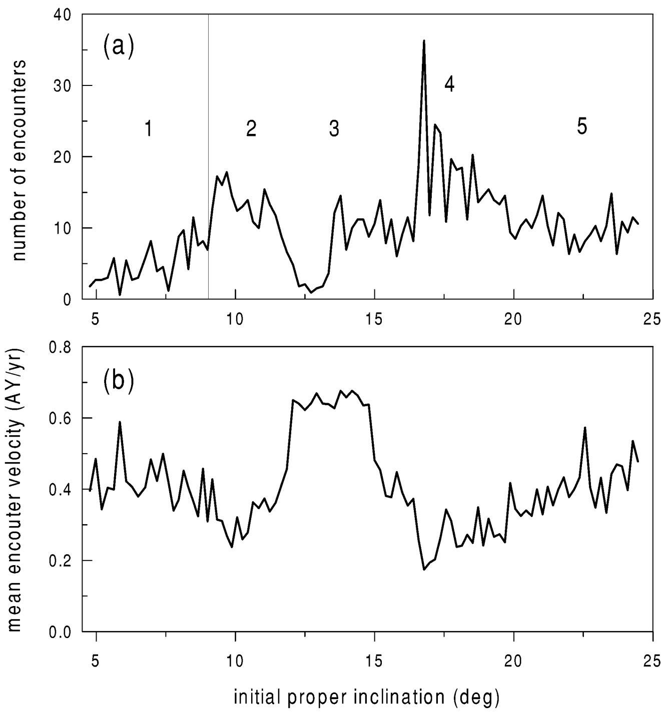

FIG. 5.—(*a*) For each test particle the number of its encounters within R_H to Pluto in the first 3×10^8 yr of simulation is shown. The simulated range of initial proper inclinations (*x*-axis) is roughly divided into five intervals with different evolutions of orbits. (*b*) The mean encounter velocity obtained by averaging over all approaches of a particle to Pluto in 3×10^8 yr. There were about 15 encounters for $15° < i < 20°$ where the mean encounter velocities were small. This is the region in which Pluto's effect is largest.

and the mean encounter velocity was about 0.4 AU yr^{-1}. This resulted in a small total deflection angle (Fig. 4*b*) and only a moderate excitation of A_σ (Fig. 4*a*). Typical evolution of orbits in this interval of inclinations is shown in Figure 6. The orbit of the test particle starting with the inclination of 7° initially exhibited motion typical for the Kozai resonance —oscillations of ω around 90°—for $t < 2.3 \times 10^8$ yr, where ω shortly moved retrogradely and then switched to the libration center at 270°. This alternation between the oscillation at 90° or 270° and the retrograde circulation of the perihelion argument is typical for the test particles at low inclinations where the size of the Kozai resonance is small. Amplitude of σ stayed small in Figure 6, and the particle survived the whole run in the 2:3 resonance. $\Delta\lambda = \lambda - \lambda_P$ showed circulation with a negative derivative and a large period in intervals of ω-libration.

5.2. $9° < i < 12°$

There were on average 15 encounters per 3×10^8 yr with the mean mutual velocity of 0.3 AU yr^{-1} for the particles starting with $9° < i < 12°$ (Fig. 5). This resulted in a relatively large total deflection angle that generally exceeded 2° in this interval. The dynamics of test particles was very interesting there and frequently resembled the pattern seen in Figure 7, where the orbital elements of the particle starting with $i = 11.°8$ are shown. $\Delta\lambda$ initially evolved retrogradely, and when $\Delta\lambda \sim 0$, it reversed and advanced with a positive derivative up to 360° when it reversed once again and repeated the cycle. At the points of reversal, the inclination either increased or decreased. Such behavior calls to mind the horseshoe orbits of the 1:1 mean motion resonance. Here, however, probably owing to the high inclination of both the perturbed body and the perturber, the orbital element coupled with $\lambda - \lambda_P$ was the inclination and not the eccentricity or the semimajor axis. Note that the orbit in Figure 7 had its mean inclination somewhat smaller than the mean inclination of Pluto, which is also unlike the usual horseshoe pattern.

In Figure 8 we show the inclination and $\Delta\lambda$ of the same test particle ($i = 11.°8$) in polar coordinates. Additional averaging of $\Delta\lambda$ and i over 5×10^8 yr has been performed in Figure 8. The horseshoe dynamics of the trajectory are now evident. It took about 7.5×10^8 yr for the test particle to complete one cycle.

The design of a perturbative treatment that would reproduce the orbit in Figure 8 is not a simple problem as there are two perturbers (Neptune and Pluto) and three resonances (2:3 with Neptune, Kozai, and 1:1 with Pluto) involved. The planar model of Yu & Tremaine (1999) does not apply here as the inclinations must be taken into account. In the next few paragraphs, we discuss a qualitative model based on the two-body approximation of encounters with Pluto.

We assume that if the distance of the test particle from Pluto (r) is larger than a small quantity R (of order of the radius of Pluto's Hill sphere: $R_H = 0.054$ AU) that the motion is determined by four outer planets (Jupiter to Neptune) and is characterized by constant proper actions, σ and ω libration, and a secular advance of the node longitude. Whenever $r < R$, we approximate the motion by the two-body (Pluto–test particle) dynamics and compute the resulting change of the heliocentric orbital elements according to the discussion earlier in this section.

The trajectory computed in this way (Fig. 9) for the same test particle as in Figure 7 ($i = 11.°8$) approximates well the exact numeric simulation. While the eccentricity remained almost constant, both the semimajor axis and inclination were changing. The inclination pattern in Figure 9 is almost identical with the mean inclination in Figure 7. Concerning the angles, while $\lambda - \lambda_P$ remained on average constant, both ω and σ evolved, under the effect of close encounters with Pluto, several tens of degrees ahead.

The behavior of the orbit in Figure 7 may be also understood on the basis of simple geometric arguments. Initially $i < i_P$ so that according to what was noted in the last paragraph of § 3, $\Omega - \Omega_P$ advances with a negative derivative, and so does $\lambda - \lambda_P$ according to equation (4). This is what happened for $t < 2 \times 10^8$ yr in Figure 7. The effect of Pluto was unimportant in this interval because the planet was angularly distant from the test particle. At $t = 2.3 \times 10^8$ yr, the difference in mean longitudes $\lambda - \lambda_P$ was small and on average positive. As $\Delta\Omega = \Omega - \Omega_P$ was also small and positive at this moment and if we suppose that $a = a_P$, $e = e_P$, and $\omega = \omega_P = 90°$, close encounters between the test particle and Pluto occurred at each revolution of their orbits in both the descending and ascending nodes. Define a fixed reference frame in the tangential plane of Pluto's node (perpendicular to Pluto's heliocentric position vector when Pluto is at node) so that the x-axis is parallel to Pluto's velocity vector and another reference frame in the same plane whose origin moves with Pluto's velocity at node

$$v = na\sqrt{\frac{1 + e^2}{1 - e^2}} \tag{5}$$

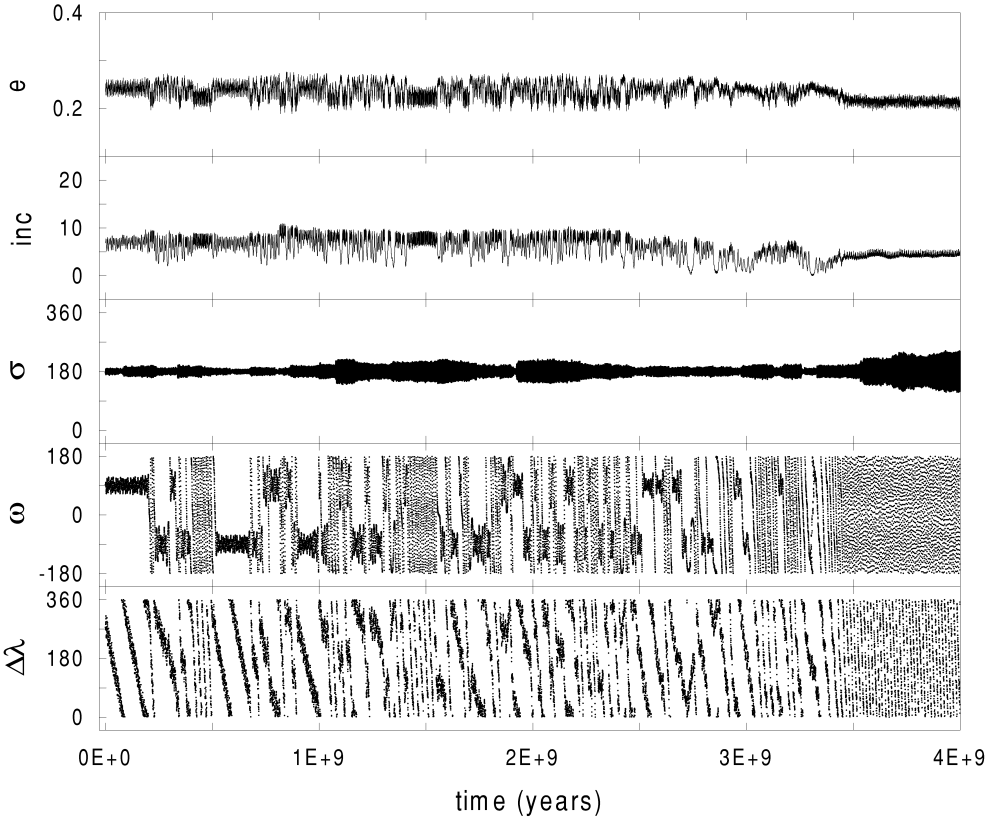

FIG. 6.—Orbit evolution of the test particle starting with $a = 39.2$ AU, $e = 0.25$, and $i = 7°$. $\sigma = 2\lambda_N - 3\lambda + \varpi$ and $\Delta\lambda = \lambda - \lambda_P$. The evolution was characterized by alternations between libration and circulation of ω, only a small excitation of A_σ and prograde circulation of $\lambda - \lambda_P$.

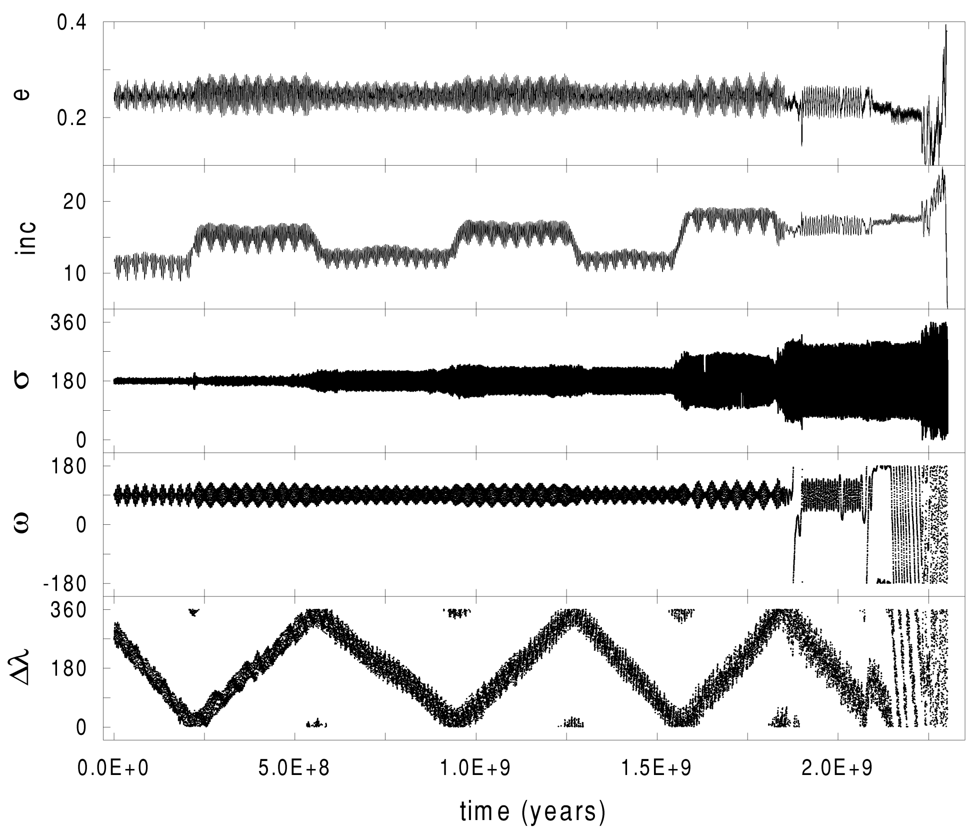

FIG. 7.—Same as Fig. 6 but for the test particle with $i = 11.8°$. The orbital evolution of this test particle was characterized by a horseshoe orbit in the 1:1 mean motion resonance with Pluto. The excitation of A_σ happened when $\lambda - \lambda_P$ reversed its sense of rotation. The perihelion argument librated with a small amplitude up to $t = 1.8 \times 10^9$ yr where A_σ increased to 120°. The particle escaped from the 2:3 resonance at $t = 2.25 \times 10^9$ yr.

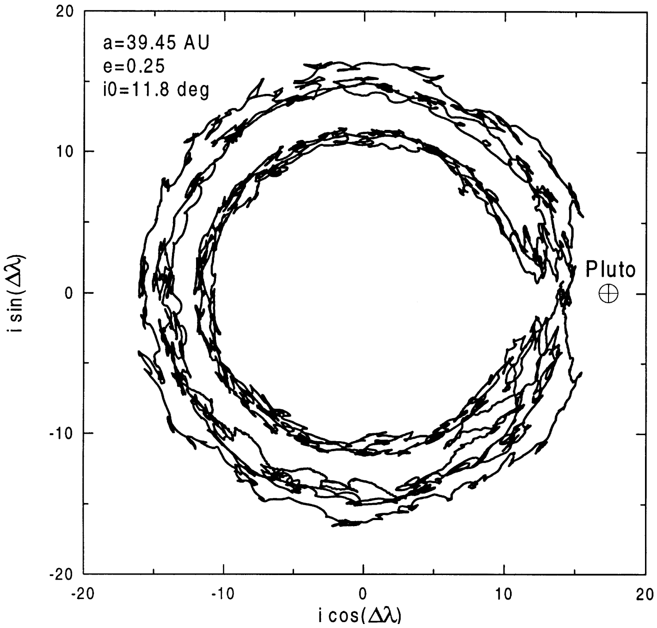

FIG. 8.—Horseshoe orbit of the same particle as in Fig. 7. Inclination and $\Delta\lambda = \lambda - \lambda_P$ are shown in polar coordinates. Unlike an ordinary horseshoe orbit, the action coupled to $\Delta\lambda$ was the inclination and not the semimajor axis or eccentricity. Note also that the mean inclination of this orbit was smaller than the inclination of Pluto.

(n being Pluto's mean motion) along the x-axis of the former and is identical with the former when Pluto is at node. Denote its axes ζ and η. Then, the components of the test particle velocity characterizing encounter in this reference system are $v_\zeta = v[\cos(i - i_P) - 1]$ and $v_\eta = v \sin(i - i_P)$. Moreover, the test particle trajectory intersects the ζ-axis at $\Delta\Omega/3$. From this geometry of the encounter in the Pluto-centric reference frame and under the assumption that the deflection angle is small, it is clear that $|i - i_P|$ will tend to zero if $\Delta\Omega > 0$. This is what happened with inclination of the test particle in Figure 7 at $t = 2 \times 10^8$ yr (see also Fig. 9, where the net effect of Pluto's encounters is shown).

If the differential rotation of nodes were fast so that the epoch of close encounters when $\Omega - \Omega_P \sim 0$ were short, the inclination change would be small, and $\Omega - \Omega_P$ would soon become negative (as for the test particle in Fig. 6—a similar argument holds for the test particle in Fig. 12, where $\Delta\Omega$

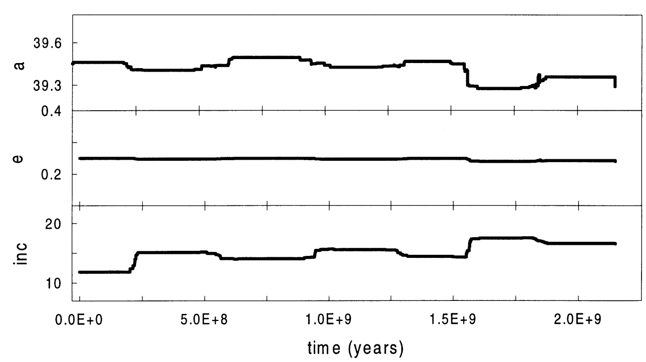

FIG. 9.—Two-body approximation of the dynamics at close encounters with Pluto. See text for details. Compare with Fig. 7 where the orbit evolution of the same test particle was computed by the exact numeric integration.

rotates with positive derivative). However, this was not the case of the test particle in Figure 7, where the inclination due to close encounters with Pluto rapidly grew, and before $\Omega - \Omega_P$ would become negative, i was already close to i_P. It was then important that Pluto (with $A_\sigma = 84°$) have a negative nodal frequency with its absolute value larger than objects with the same orbital parameters but smaller A_σ. This means that when $i = i_P$ for the test particle in Figure 7, both $\Omega - \Omega_P$ and (according to eq. [1]) $\lambda - \lambda_P$ must have had a positive time derivative. This is what we see in Figure 7 in the interval $2.5 < t < 5 \times 10^8$ yr, where Pluto's effect is once again negligible.

The geometry of encounters with $\Delta\Omega < 0$ at $t = 5.5 \times 10^8$ yr is different, and, as an analysis of the encounter in the tangential plane shows, $|\Delta i|$ must increase in this case. Consequently, when i sufficiently decreases in several encounters with Pluto $\Omega - \Omega_P$ reverses its sense of the rotation.

A quantitative computation of the orbital changes in the Öpik approximation of encounters is, however, strongly dependent on the distance R, where one chooses to approximate the motion by the two-body model. For larger values of R the computed change of orbital elements is large, while for small values of R, the computed orbital change is small. The development of a quantitative perturbative model of Neptune-Pluto-Plutino interaction is an interesting area for future research. The circular planar model of Yu & Tremaine (1999) is not realistic enough to account for the real evolution of Plutino orbits.

5.3. $12° < i < 15°$

Several trajectories in the interval $12° < i < 15°$ (Fig. 5*a*—interval 3) were close to the leading or trailing Lagrangian points of the Sun–Pluto–test particle system (tadpole orbits). Pluto's orbit is noncircular, and the triangular Lagrangian points are not necessarily placed at 60° from Pluto. The orbit in Figure 10 (initially $i = 14.^\circ4$) is an example of motion near the trailing stationary point. Most of the time the orbit was protected from close encounters with Pluto, and only a few high-velocity approaches did not enlarge A_σ above the instability limit. The test particle in Figure 10 survived the whole run. The orbits near the Lagrangian points were, however, susceptible to small orbital changes, and they frequently switched to horseshoe orbits in our simulation, where the interaction with Pluto led to the important A_σ excitation.

5.4. $15° < i < 20°$

The initial inclinations in the range $15° < i < 20°$ (Fig. 5*a*) led to a variety of different orbital behaviors. The relative inclinations to Pluto's orbit were small when the nodes became aligned in the simulation and there were more than 15 encounters in 3×10^8 yr with the mutual velocity as low as 0.2 AU yr^{-1} in this interval of initial inclinations (Fig. 5). Large deflection angles (Fig. 4*b*) of the low-velocity encounters caused significant alterations of orbits, excitation of A_σ, and escapes to Neptune-crossing trajectories. The evolution of the test particle in Figure 11 (initial $i = 16.^\circ8$) showed an alternation between all three orbital modes of the 1:1 mean motion resonance with Pluto: the horseshoe orbit and the tadpole orbits near the trailing and leading Lagrangian points. A large excitation of A_σ already occurred for this test trajectory at the beginning of the integration, and the particle escaped from the resonance at

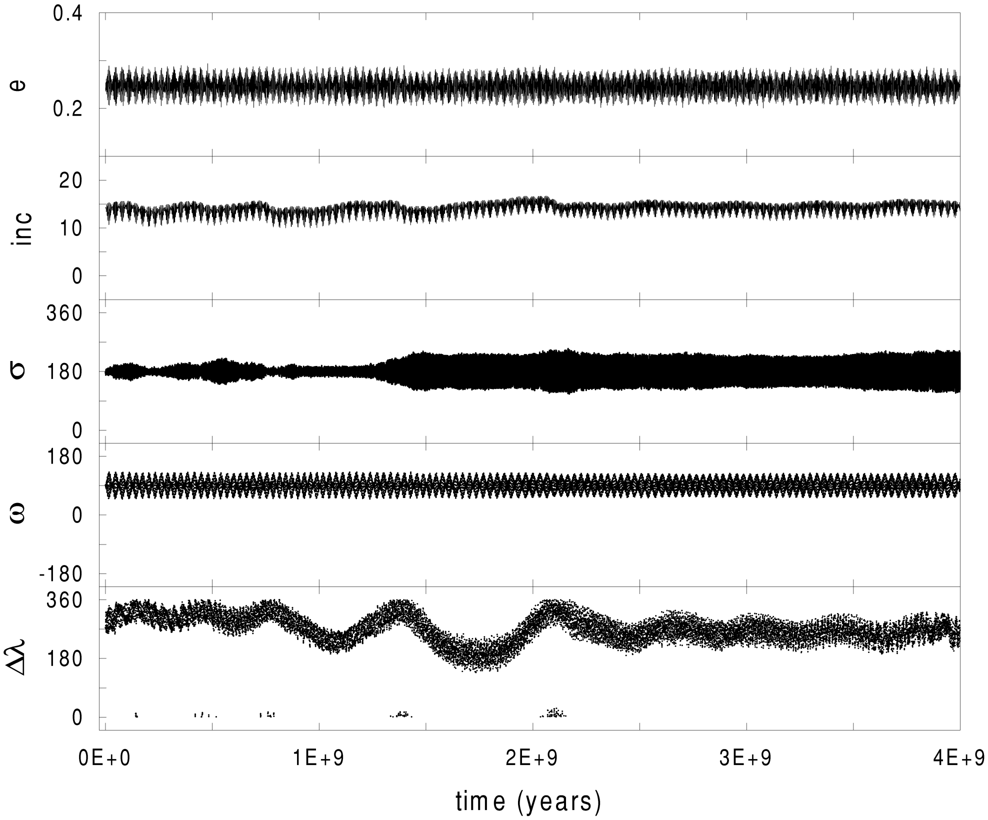

FIG. 10.—Same as Fig. 6 but for the test particle with $i = 14\overset{\circ}{.}4$. This trajectory is near the trailing Lagrangian point of the Sun–Pluto–test particle system. Its resonant amplitude was moderately excited at $t = 1.4 \times 10^9$ yr, where $\lambda - \lambda_P$ was close to zero. A_ω of the orbit stayed almost constant, and the test particle survived the whole run in the Kozai resonance.

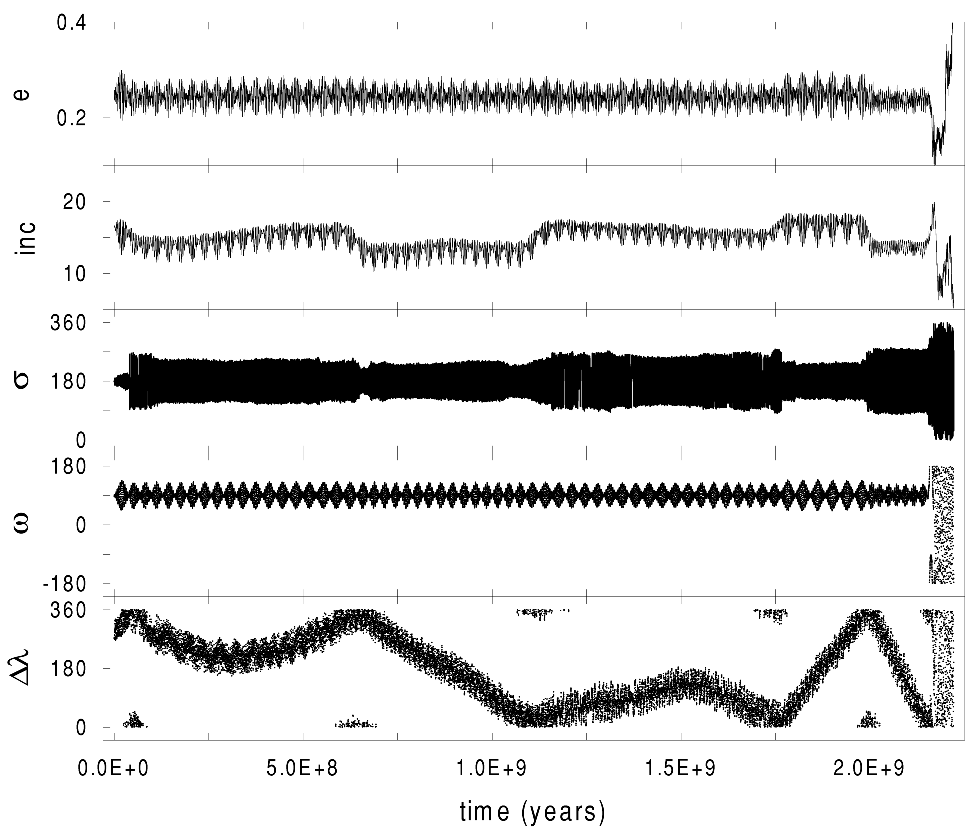

FIG. 11.—Same as Fig. 6 but for the test particle with $i = 16\overset{\circ}{.}8$. The trajectory is near the trailing Lagrangian point with respect to Pluto's orbit up to $t = 6 \times 10^8$, where it migrates to the leading point and later performs one cycle of the horseshoe orbit ($1.75 < t < 2.2 \times 10^9$ yr). It escapes from the resonance at 2.2×10^9 yr.

2.2×10^9 yr and was deactivated at 2.25×10^9 yr owing to a very close encounter with Neptune.

5.5. $i > 20°$

The test particles with $i > 20°$ had a prograde circulation of $\lambda - \lambda_P$, and most of them escaped from the 2:3 resonance after their A_σ was significantly excited by close encounters with Pluto. An example of motion is shown in Figure 12 for the test particle with an initial inclination of 23°. Note the large time interval of about 2×10^8 yr that the test particles had passed at the separatrix of the 2:3 resonance ($A_\sigma \sim 180°$). This shows the possible existence of long-lived objects with large A_σ.

6. ORBITAL DISTRIBUTION OF THE SURVIVING POPULATION

Concerning the test particles surviving 4×10^9 yr in the 2:3 resonance in our experiment, we show in Figure 13*a* their smoothed resonant amplitude (averaged over 1° interval of the initial inclination). $A_\sigma(4 \times 10^9$ yr) is denoted by a solid line, and $A_\sigma(0)$ is shown for reference by a dotted line. The excitation of the resonant amplitude is important: the average $A_\sigma(4 \times 10^9$ yr) over all test particles is about 80°. The final resonant amplitude depends on the initial inclination. While for the test particles initially at $i < 10°$ A_σ $(4 \times 10^9$ yr) is usually smaller than 70°, for a larger initial inclination the excitation is larger. The small depression on the curve of $A_\sigma(4 \times 10^9$ yr) at about 15° is a consequence of the fact that several test particles with this initial inclination passed long time intervals near the Lagrangian points, being phase-protected from close encounters to Pluto.

Another important result of the simulation is that a few test particles were found to be on ω-librating orbits in the Kozai resonance at $t = 4 \times 10^9$ yr. The test particles were chosen so that initially $A_\omega(0) < 25°$ with an average of 10°, and at the end of the run, there were only 14 test particles with $A_\omega < 70°$. Seven of the particles surviving in the Kozai resonance started with inclinations in the interval $12.°5 < i < 16.°5$ and spanned long time intervals on tadpole orbits of the 1:1 mean motion resonance with Pluto. Five other test particles with $A_\omega(4 \times 10^9$ yr) $< 70°$ had an initial inclination larger than 22°. The fact that only 14% of the test particles are found in the Kozai resonance at the end of simulation can be related to the lack of observed Plutinos on orbits similar to Pluto's orbit. We conjecture that the gap observed in the distribution of known Plutinos at the Kozai resonance in Figure 1*b* may be a consequence of Pluto's sweeping effect.

In Figure 13*b* we show the initial (*dashed line*) and final distribution of test particles versus the resonant amplitude A_σ. At $t = 4 \times 10^9$ yr, the number of particles per 10° of A_σ varies between three and eight for $A_\sigma > 25°$ and is zero for $A_\sigma < 25°$. Eleven test particles that have not been deactivated during the run had $130° < A_\sigma(4 \times 10^9$ yr) $< 170°$ in spite of the motion at these resonant amplitudes being chaotic and unstable on at most several 10^8 yr. Consequently, there might be presently many Plutinos on such transitional

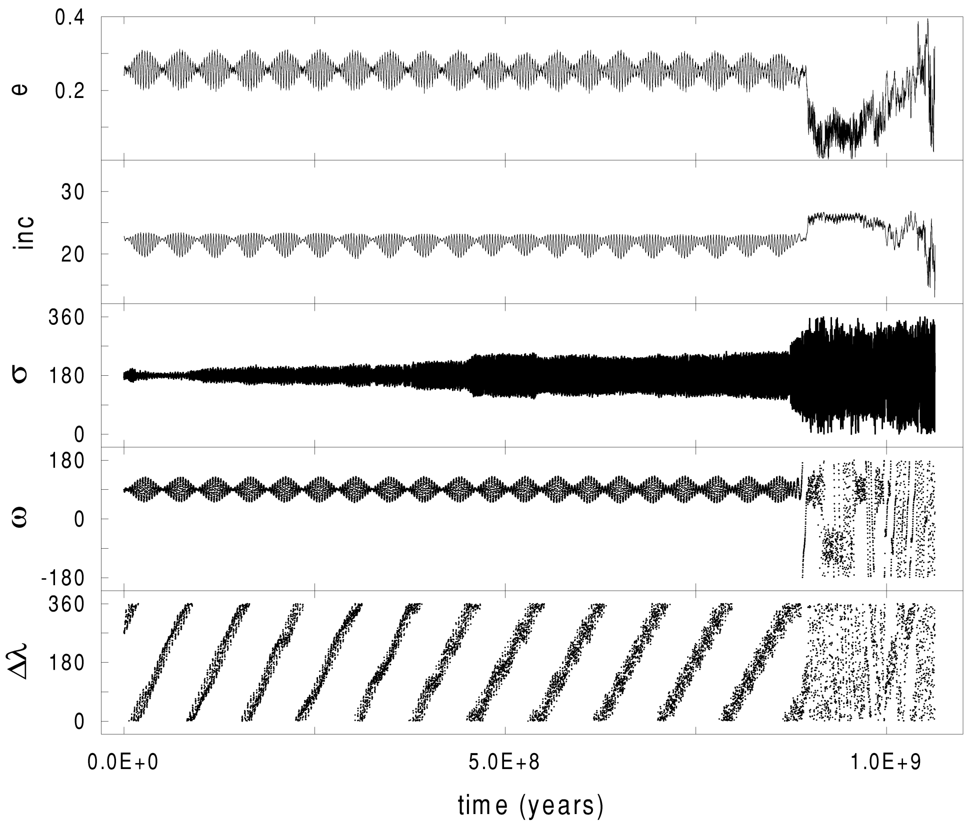

FIG. 12.—Same as Fig. 6 but for the test particle with $i = 24°$. $\lambda - \lambda_P$ evolved with a positive derivative, and each time when $\lambda - \lambda_P = 0$ the resonant amplitude A_σ somewhat increased. The particle was removed from the resonance at 8.7×10^8 yr and was deactivated at 1.07×10^9 yr as its heliocentric distance exceeded 100 AU.

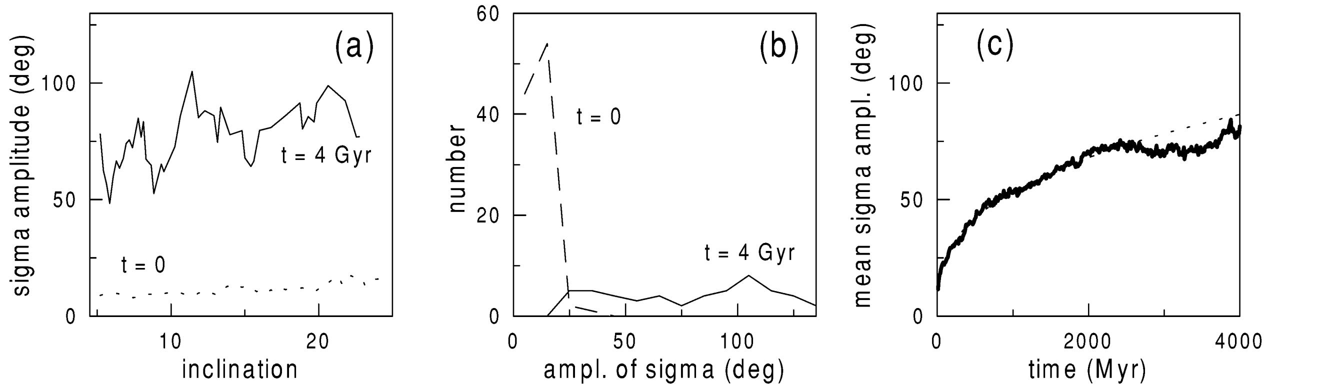

FIG. 13.—(*a*) Mean A_σ (average over a 10° window in inclination) for $t = 0$ (*dotted line*) and $t = 4 \times 10^9$ yr (*solid line*) for the test particles surviving the whole run. (*b*) Distribution of the test particles with respect to their A_σ. The number of test particles within a 10° interval of A_σ is shown for $t = 0$ (*dashed line*) and $t = 4 \times 10^9$ yr (*solid line*). (*c*) Evolution of $A_\sigma(t)$ calculated as average over all surviving particles at time *t*. The final excitation is about 80°. The dotted line in (*c*) is a least-squares fit. See text for details.

orbits with $A_\sigma > 130°$, and the long-term orbital stability is not a necessary condition of correct orbital elements computation from observations.

Figure 13*c* shows the evolution of the mean libration amplitude of the surviving population with time. The solid line is the average of $A_\sigma(t)$ over the test particles that had survived the integration up to the time *t* (not considering the test particles that had already escaped from the resonance). The power time dependence αt^β, fitted by the least-squares method to average $A_\sigma(t)$, is defined by $\alpha = 4.83$ and $\beta = 0.344$ (dotted line in Fig. 13*c*). The initially low resonant amplitude increases to about 80° at $t = 4 \times 10^9$ yr.

7. EXPLORING PLUTO'S EFFECT FOR $e \neq 0.25$

The experiment in the previous section has been performed with both initial A_σ and A_ω small choosing the resonant semimajor axis and $e = 0.25$ for the initial orbital elements. Here we explore Pluto's effect in the 2:3 Neptune resonance also for different initial eccentricities.

One-hundred one test particles have been placed at $a = 39.2$ AU, $i = 17°$, and with eccentricity between 0.15 and 0.35 (0.002 step). The initial angles, integration parameters, and integration procedure were exactly the same as in the run in the previous section. The total integration time span was 2×10^9 yr.

Also for these initial conditions, many test particles escaped from the 2:3 resonance. By $t = 2 \times 10^9$ yr, 34 test particles had already left the resonance. A linear extrapolation of a cumulative number of escapes to 4×10^9 yr suggests removal of about 60% of test particles. Recall that also in this case, the escape of test particles must be attributed to the effect of Pluto, as other planets do not cause any secular trends of the resonant orbits with $A_\sigma < 50°$.

Figure 14*a* shows $A_\sigma(0)$ (*solid line*) and $A_\sigma(2 \times 10^9$ yr) (*shadow bars*). Most of the escaping test particles were initially in the interval $0.2 < e < 0.32$, which is the approximate width of Kozai resonance at $i = 17°$ (Morbidelli et al. 1995). For low ($e < 0.2$) and high ($e > 0.32$) eccentricities, the excitation of A_σ was smaller, and fewer test particles leaked from the 2:3 resonance at these eccentricities. The total deflection angle shown in Figure 14*b* is well correlated with the number of escapes. It is larger than 1° for most of the escaping trajectories in the $0.2 < e < 0.32$ interval.

The number of encounters within R_H to Pluto in 3×10^8 yr shows an interesting profile (Fig. 15*a*). There were usually fewer than five encounters for $e < 0.2$ with the mean velocity of 0.4 AU yr^{-1}. At $e > 0.2$, the number of encounters increases with increasing eccentricity up to the peak of about 20 encounters (on average) at $e = 0.25$. This eccentricity coincides with the libration center of the Kozai resonance. The mean encounter velocity is only 0.2 AU yr^{-1} for $e = 0.25$. The relatively large number of encounters combined with low encounter velocity led to large orbital changes of the test particles starting with $0.2 < e < 0.32$ and the excitation of their resonant amplitudes A_σ (Fig. 14*a*). This showed that most orbits in the Kozai resonance (and

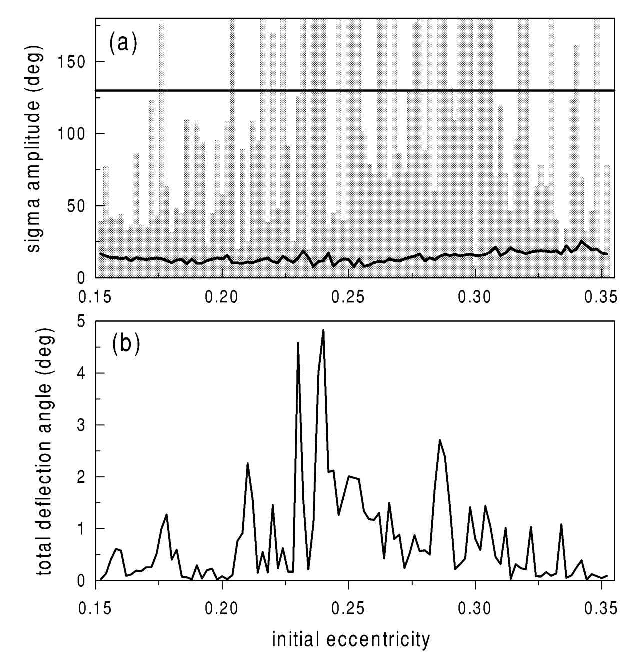

FIG. 14.—Same as Fig. 4 but for the run of 101 test particles initially with $i = 17°$. Most of the escapes happened for $0.2 < e < 0.32$, where also the cumulative deflection angle calculated from encounters with Pluto was large. This region roughly corresponds to the orbits in the Kozai resonance.

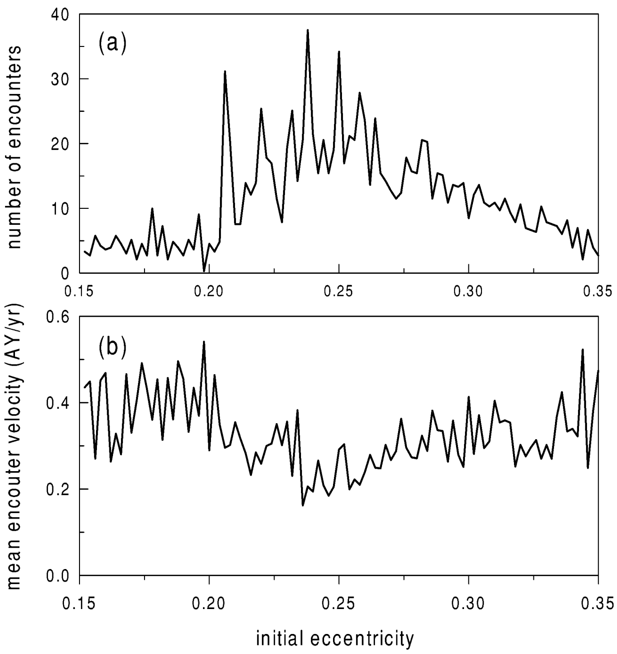

FIG. 15.—Same as Fig. 5 but for the run of 101 test particles initially with $i = 17°$. The number of encounters within R_H to Pluto is the largest at $e = 0.25$, where about 20 encounters happen in 3×10^8 yr. The encounter velocity is about 0.2 AU yr^{-1} for this eccentricity.

not only those at its libration centers) were efficiently modified by Pluto's influence. The gap in the orbital distribution of Plutinos should be roughly of the size of the Kozai resonance.

The surviving 67 test particles at 2×10^9 yr had the mean A_σ as large as 66° (Fig. 16*a*). Initially (dotted line in Fig. 15*a*) the mean A_σ was 14°. The number of test particles in 10° of A_σ versus A_σ is both initially (*dashed line*) and at 2×10^9 yr (*solid line*) shown in Figure 16*b*. There were initially 80 test particles with $10° < i < 20°$. The profile at 2×10^9 yr is characterized by a peak density of test particles at the amplitude of about 45° (mainly formed by the test particles starting with $e < 0.25$ and $e > 0.3$) and a number of orbits with A_σ largely excited. There are about five particles per 10° of A_σ for $70° < A_\sigma < 110°$.

The mean resonant amplitude increased considerably with time (Fig. 16*c*). The solid line in this figure is the average over the surviving particles. The dotted line is the least-squares fit that results in the same power dependence on time as the power fit in Figure 13*c* [$A_\sigma(t) \sim t^{1/3}$]. The extrapolation to 4×10^9 yr shows that the resonant amplitude of the surviving test population at 4×10^9 yr should be about 80°. It could be, however, a little smaller if the deceleration trend observed shortly before 2×10^9 yr would continue also for $t > 2 \times 10^9$ yr. In any case a large excitation of A_σ can be expected also for the orbits with $e \neq 0.25$

8. CONCLUSIONS

Pluto's orbit is locked in the Kozai resonance in contrast with almost all observed Plutinos. According to the analysis in this work, this observation result can be explained by Pluto's effect on Plutinos. The orbits starting with the low amplitude of ω oscillations are, for a wide range of initial inclinations, ejected from the Kozai resonance on the 10^9 yr timescale. As the opposite process (i.e., evolution into the Kozai resonance) is less effective, a gap must have been formed around Pluto's orbit in eccentricity and inclination. This gap is actually observed in the distribution of known Plutinos.[3]

The only objects surviving long time intervals in the Kozai resonance are usually protected from close encoun-

[3] It is certainly a possibility that the lack of Plutinos in the Kozai resonance is related to a slow primordial migration of Neptune's orbit suggested by Malhotra (1996). If the evolution of a captured 2:3 resonant object toward larger eccentricities is envisaged as a consequence of slow outward migration of the 2:3 Neptune resonance, this object encounters the lower separatrix of the Kozai resonance at an eccentricity that depends both on A_σ and inclination (Fig. 1). The theory of adiabatic capture may be applied in this case, and the probability of capture in the Kozai resonance can be computed (a simple numeric experiment can also yield an answer). If the capture probability is near 1, the gap is not primordial. If the probability is near 0, the primordial gap could have been formed, since most bodies should have avoided the Kozai resonance during their migration. We nevertheless believe that collisions (such as the one in which the Pluto-Charon binary has been presumably formed) must have resupplied new objects in the region of the Kozai resonance since then.

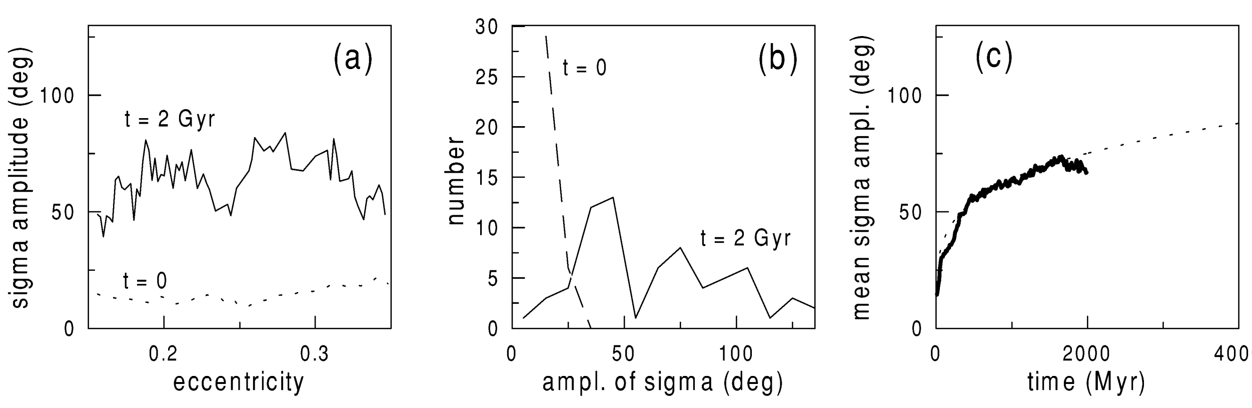

FIG. 16.—(*a*) Mean A_σ (average over a 0.01 window in eccentricity) for $t = 0$ (*dotted line*) and $t = 2 \times 10^9$ yr (*solid line*) for the test particles surviving the whole run. The experiment with $i = 17°$. (*b*) Distribution of the test particles with respect to their A_σ. The number of test particles within a 10° interval of A_σ is shown for $t = 0$ (*dashed line*) and $t = 2 \times 10^9$ yr (*solid line*). In fact all test particles had the initial $A_\sigma < 30°$. (*c*) Evolution of mean $A_\sigma(t)$ calculated as average over all surviving particles at time *t*. The excitation at 4×10^9 yr suggested by the extrapolation (*dotted line*) is about 80° . The dotted line in (*c*) is a least-squares fit.

ters with Pluto being trapped on tadpole orbits in the 1:1 resonance with the planet. There should be a number of Pluto's Trojans with mean inclinations of about 15°. As we have confirmed by a numeric simulation, 1997 QJ4 is the first observed example of this dynamical class. $\lambda - \lambda_P$ of 1997 QJ4 has been locked at 80° for at least the last 10^9 yr. Such an orbit makes of this object a good candidate for a body dynamically related to the Pluto-Charon binary formation event (Stern, Canupt, & Durda 1999), and the determination of physical properties of its surface by spectral observations would be interesting. Of course, it is equally probable that 1997 QJ4 is just a sample of a dynamically primordial population formed in the Kozai resonance or a collisionally injected body.

Another interesting class of orbital evolution in the 1:1 resonance with Pluto found in our simulations is a horseshoe orbit in which $\lambda - \lambda_P$ is coupled with inclination (Fig. 7). Such orbits are, however, very susceptible to Pluto's perturbation and usually do not survive on the age of the solar system because of the enlargement their resonant amplitude A_σ. The horseshoe orbits present the highest frequency and lowest mutual velocity of encounters with Pluto. Most of the trajectories closely encountering Pluto have the horseshoe dynamics.

An important effect of Pluto is its large excitation of the libration amplitudes in the 2:3 resonance. The surviving population of Plutinos with the primordial inclination larger than 8° should have had its mean A_σ increased to about 80° on the solar system age. The excitation of low-eccentricity orbits is smaller and accounts for an estimated 10° increase of mean A_σ per 10^9 yr. The change of A_σ for a Plutino on the low-inclination orbit can be, however, substantially larger in specific case. The traces of A_σ excitation driven by Pluto can actually be observed in the 2:3 resonance as there exists a lack of observed low-A_σ Plutinos (Fig. 2).

The excitation of A_σ by close encounters with Pluto leads to the escape from the 2:3 Neptune resonance when A_σ increases beyond the instability limit ($\sim$120°). We estimate that about 50% of dynamically primordial objects in the Kozai resonance had been removed from the 2:3 resonance by this mechanism. For $i > 8°$, even more than 70% should have had their A_σ increased above the instability limit after 4×10^9 yr. Consequently, the population of Plutinos must have suffered a significant mass loss in the past.

Pluto-induced excitation of the resonant amplitude and evolution of Plutinos onto Neptune-crossing orbits contributes to the flux of short-period comets from the trans-Neptunian region. We estimate that the flux rate from $i > 8°$ orbits at about 1% of such 2:3 resonant population per 10^8 yr, which is about of the same value as the flux expected from the marginally unstable region without Pluto (Morbidelli 1997). For $i < 8°$, the expected Pluto-induced flux should be a factor of 2–5 smaller. Consequently, the marginally unstable region is continuously resupplied from low-A_σ region, and a large part of the 2:3 resonance is an active source of short period comets.

These were the main conclusions. In the following, we briefly discuss two issues that are related to the work presented here and are of possible interest for future research.

According to Stern & Yelle (1999), *HST* observations had shown that Charon's eccentricity is nonzero, with a best estimated value of 0.0076. The fact that the orbit is not precisely circular indicates some disequilibrium forces have disturbed it from the exact value of zero expected from tidal evolution. It is most likely that the disturbance causing this is generated by occasional close encounters between the Pluto-Charon system and one of the 100 km or larger diameter bodies now known to orbit with Pluto in the Edgeworth-Kuiper belt.

The number of encounters within a distance R to Pluto on time interval t is proportional to $P_i N R^2 t$, where N is the number of bodies ($\sim$10,000 with diameter larger than 100 km according to Jewitt et al. 1998). The intrinsic probability P_i (Davis & Farinella 1997) may be computed from our experiment. As there are on average 10 encounters within R_H to Pluto in 3×10^8 yr, the estimated intrinsic probability is

$$P_i = 5 \times 10^{-22}\ \mathrm{km}^{-2}\ \mathrm{yr}^{-1}\ . \quad (6)$$

Setting $R = 40{,}000$ km, which is about double the semimajor axis of Charon's orbit, there is about 1.3 such encounters per 10^8 yr. The possible excitation of Charon's eccentricity by a near fly-by of a 100 km body and the subsequent tidal relaxation of the orbit are surely interesting areas for future studies.

The second interesting issue that emerged with the results presented in this paper is whether the excitation of A_σ works in one direction (i.e., Pluto enlarged A_σ of Plutinos) or whether also the opposite effect (i.e., Plutinos enlarged A_σ of Pluto) might be significant.

Assuming the 7000–14,000 objects with diameters larger than 100 km in the 2:3 Neptune resonance (Jewitt et al. 1998), their total mass (0.01–0.02 of Earth's mass) exceeds Pluto's mass (which is about 0.002 of Earth's mass) by a factor of 5–10. Now, if Pluto has a considerable effect on these bodies in 4×10^9 yr as shown in this paper, the resonant bodies must have at least an equally large effect on Pluto. We conjecture that Pluto's large resonant amplitude ($\sim$80°—equal to the final average excitation observed in our simulations of test particles on initially inclined orbits) resulted—at least partially—from the mutual interaction with resonant bodies.

This subject is closely related to the work of Levison & Stern (1995), but the reasoning is somewhat different. Instead of trying to stabilize Pluto's orbit in the dense primordial Kuiper belt by scattering it to a stable orbit inside the resonance (in time intervals of order of 5×10^7 yr), assume the present Kuiper belt density (which is about 1% of the primordial), and compute the effect of gravitational scattering on Pluto in last 4×10^9 yr. Owing to lower density, the frequency of encounters will be a factor of 100 smaller than in the primordial belt, but the interval is 100 times longer than that in Levison & Stern (1995). Consequently, the net effect in such an interaction can be about the same, and the amplitudes of Pluto's resonant angle and perihelion argument may be expected to change by several to several tens of degrees (as in Fig. 8 of Levison & Stern 1995). Pluto's orbit could well have been different in the past.

Most of the numeric simulations have been performed using the computer resources of the São Paulo University computer center LCCA in the frame of the project "Asteroid Resonant Dynamics and Chaos." This research was sponsored by the São Paulo State Science Foundation FAPESP.

REFERENCES

Brown, E. W., & Shook, C. A. 1966, Planetary Theory (New York: Dover)
Cohen, C. J., & Hubbard, E. C. 1965, AJ, 70, 10
Davis, D. R., & Farinella, P. 1997, Icarus, 125, 50
Duncan, M. J., Levison, H. F., & Budd S. M. 1995, AJ, 110, 3073
Duncan, M. J., Quinn, T., & Tremaine, S. 1988, ApJ, 328, L69
Edgeworth, K. E. 1949, MNRAS, 109, 600
Fernández, J. A. 1980, MNRAS, 192, 481
Henrard, J. 1990, Celest. Mech. Dyn. Astron., 49, 43
Holman, M., & Wisdom, J. 1993, AJ, 105, 1987
Jewitt, D. C., & Luu, J. X. 1993, Nature, 362, 730
Jewitt, D. C., Luu, J. X., & Trujillo, C. 1998, AJ, 115, 2125
Kinoshita, H., & Nakai, H. 1984, Celest. Mech. Dyn. Astron., 34, 203
Knežević, Z., Milani, A., Farinella, P., Froeschle, Ch., & Froeschle, C. 1991, Icarus, 93, 316
Kozai, Y. 1962, AJ, 67, 591
Kuiper, G. P. 1951, in Proc. Astrophysics: A Tropical Symposium, On the Origin of the Solar System, ed. J. A. Hynek (New York: Mc Graw-Hill), 357
Levison, H. F., & Duncan, M. J. 1993, ApJ, 406, L35
———. 1994, Icarus, 108, 18
———. 1997, Icarus, 127, 13
Levison, H. F., & Stern, S. A. 1995, Icarus, 116, 315
Levison, H. F., Stern, S. A., & Duncan, M. J. 1999, Icarus, submitted
Malhotra, R. 1993, Nature, 365, 819
Malhotra, R. 1996, AJ, 111, 504
Milani, A., Nobili A. M., & Carpino, M. 1989, A&A, 96, L1
Morbidelli, A. 1997, Icarus, 127, 1
Morbidelli, A., & Nesvorný, D. 1999, Icarus, 139, 295
Morbidelli, A., Thomas, F., & Moons, M. 1995, Icarus, 118, 322
Nesvorný, D., & Ferraz-Mello, S. 1997, Icarus, 130, 247
Nesvorný, D., & Roig, F. 2000, Icarus, submitted
Öpik, E. J. 1976, in Interplanetary Encounters, ed. Z. Kopal & A. Cameron (New York: Elsevier)
Petit, J. M., Morbidelli, A., & Valsecchi, G. B. 1999, Icarus, 141, 367
Quinlan, G. D., & Tremaine, S. 1990, AJ, 100, 1694
Quinn, T., Tremaine, S., & Duncan, M. 1991, AJ, 101, 2287
Stern, S. A., Canup, R., & Durda, D. D. 1999, preprint
Stern, S. A., & Yelle, R. V. 1999, in The Encyclopedia of the Solar System, ed. T. V. Johnson, P. R. Weissman, & L. A. McFadden (Academic Press), Chapter 22
Sussman, G. J., & Wisdom J. 1988, Science, 241, 433
Thomas, F. 1998, Ph.D. thesis, Observatoire de Paris
Williams, J. G., & Benson, G. S. 1971, AJ, 76, 167
Yu, Q., & Tremaine, S. 1999, AJ, 118, 1873